

## **DESIGN AND EVALUATION OF A ROBUST COMPLIANT GRASPER USING SHAPE DEPOSITION MANUFACTURING**

**Aaron M. Dollar**

Division of Engineering and Applied Sciences  
Harvard University  
Cambridge, MA 02138, USA  
adollar@deas.harvard.edu

**Robert D. Howe**

Division of Engineering and Applied Sciences  
Harvard University  
Cambridge, MA 02138, USA  
howe@deas.harvard.edu

### **ABSTRACT**

Robustness is a limiting factor in experimental development of multifingered robot hands: the expense and fragility of these hands precludes casual experimentation, restricting the type of experimental tasks that can be reasonably attempted and slowing implementation due to the need for careful validation of programs. In this paper, we describe the design, fabrication, and evaluation of a novel compliant robotic grasper and demonstrate that polymer-based Shape Deposition Manufacturing allows for the construction of fingers with the functionality of conventional metal prototypes but with robustness properties that allow for uncertainty in object location and large impact forces.

*Keywords:* Robotic Grasping, Robot Hand Design, Shape Deposition Manufacturing, Rapid Prototyping, Unstructured Environments

### **INTRODUCTION**

Compliance conveys several advantages for robotic grasping. In unstructured environments, sensing uncertainties are large and target object size and location may be poorly known. Finger compliance allows the gripper to conform to a wide range of objects while minimizing contact forces. Robot joint compliance or stiffness has often been considered in the context of active control, where active control uses sensors and actuators to achieve a desired force-deflection relationship [1-3]. In contrast, passive compliance, implemented through springs in robot joints, offers additional benefits, particularly in impacts, where control loop delays may lead to poor control of contact forces [4-8]. The reduced need for the sensing required to create active compliance can also lead to lower implementation costs.

In previous work, we examined the optimization of the design of simple two-fingered grippers with passive springs in the joints [9]. This study showed that for a particular set of joint stiffnesses and rest angles, the widest range of uncertainty in object size and location could be allowed for. Contact forces

were also minimized at approximately the same gripper configuration. In addition to simulation studies, these results were confirmed with experimental tests using a reconfigurable gripper with metal links and joint springs [10].

In this study, we explore the benefits of using Shape Deposition Manufacturing for constructing this type of simple two-fingered gripper for unstructured environments [11,12]. This process uses polymers to simultaneously create the rigid links and compliant joints of the gripper, with embedded sensing and actuation components. In addition to simplifying the construction process, the result is an extremely robust gripper, fully functional after high impact loads and other forces due to unintended contact. In this paper we begin with a description of the shape deposition manufacturing process and the design and manufacture of the prototype gripper. We then present experimental evaluation of the gripper, including informal evaluation of the gripper's robustness and a quantitative study of its performance in grasping, in comparison to both simulation results and the metal prototype's performance.

### **DESIGN**

#### *Shape Deposition Manufacturing*

To fabricate our experimental grasper, we used an emergent manufacturing technique called Shape Deposition Manufacturing (SDM) [11,12]. This rapid prototyping process involves a cycle of deposition of part material and shaping, building up the part in distinct layers, and resulting in the concurrent manufacture and assembly of the part. In this way, the part can be manufactured in multiple sections or layers, allowing manipulation of the internal parts of the final structure. A diagram detailing the process is shown in Fig. 1 and an example use of the process with detailed steps is laid out in the next section.

This process has a number of advantages over other prototyping techniques. The deposition of part material allows components to be embedded into the part during production, eliminating the need for fasteners, and reducing the likelihood

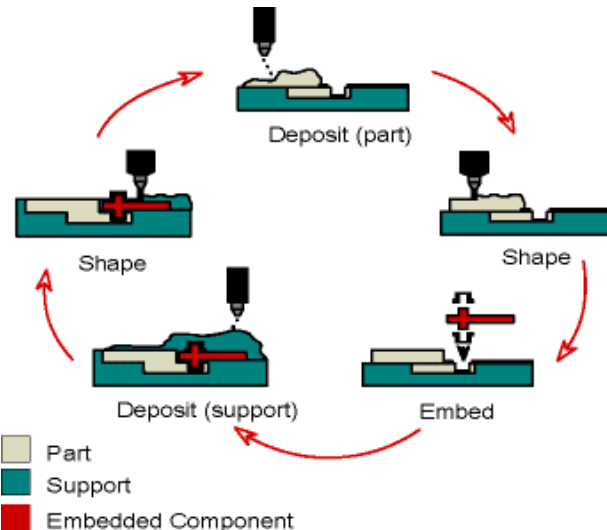


Fig. 1 Diagram explaining the SDM process. Courtesy of Mark Cutkosky.

of damage to the component by encasing it within the part structure. This is a particularly desirable property for the inclusion of fragile components such as sensors, greatly increasing the robustness of the part. Also, depositing the part in layers permits the use of dissimilar materials, allowing for variation of mechanical properties within the same part. This property can be utilized to create complex mechanisms from a single part [13,14].

Due to its relative simplicity, custom tooling is not required to realize the SDM process. Complex part geometries can be attained using common computer numerical controlled (CNC) mill machines.

#### *Grasper Design and Fabrication*

The diagram in Fig. 2 shows the steps of the SDM process used to produce our compliant grasper fingers. Pockets corresponding to the shape of the stiff links of our fingers are machined into a high-grade machine wax (Freeman Manufacturing and Supply Co., Akron, Ohio, USA). The components in panel A are put into place in the pockets (panel B), and the polymer resin poured. Modeling clay is used to dam any areas needing to be blocked from the resin. After the layer cures, a second group of pockets is machined (both into the support wax and the stiff resin) and dammed (panel C). The polymer resins for the compliant finger joints (white) and soft fingerpads (clear) are then poured (panel D) and allowed to cure. The block is then faced off to level the surface and remove surface flaws (panel E), and the completed fingers removed from the wax support material. The entire process takes approximately 30 hours to complete, only 4 of which require human supervision.

The polymers chosen are two-part industrial polyurethanes (Innovative Polymers, St. Johns, Michigan, USA). The materials for the soft fingerpads, compliant joints, and stiff links are IE35A, IE90A, and IE72DC, respectively. Degassing at  $-737\text{mmHg}$  ( $-29^\circ\text{Hg}$ ) was sometimes necessary to prevent voids in the cured resins. Table I shows material properties of these three polyurethanes as provided by the manufacturer.

TABLE I  
MATERIALS SPECIFICATIONS

	IE-35A	IE-90A	IE-72DC
Hardness	30-40A	85-95A	75-85D
Tensile Strength ASTM D-638 (ksi)	0.4	1.8	10
Elongation at Break	470%	100%	2%
Tear Strength ASTM D-624 (pil)	50	250	N/A
Flex Modulus ASTM D-790 (ksi)	N/A	N/A	325
Ultimate Flex Strength D-790 (ksi)	N/A	N/A	13

TABLE II  
NOMENCLATURE

parameter	definition
$\varphi_1, \varphi_2$	spring rest link angles
$\theta_1, \theta_2$	angular deflections from $\varphi_1$ and $\varphi_2$
$k_1, k_2$	joint stiffness values
$k_T$	total stiffness ( $k_1, k_2 / k_1+k_2$ )
$x_c$	distance from object center to the grasper centerline
$r$	object radius
$l$	grasper link length
$f_R$	resultant contact force = $\sqrt{f_T^2 + f_N^2}$
$f_T$	contact force tangential to the link surface

Figure 3 diagrams the parts of the SDM finger. The concave side of each link contains a soft fingerpad to maximize friction and increase grasp stability [15,16]. The cream-colored sections are the compliant joint flexures, designed to be compliant in the plane of finger motion, and stiff out of plane. The joints as designed have stiffnesses of 0.0421 Nm/rad and 0.224 Nm/rad for the proximal and distal joints, respectively.

Conveniently, the polymer used for the stiff links is transparent, allowing the embedded components to be clearly seen (also see Fig 2, panel A). Joint angle sensing is accomplished by embedding a low output impedance linear hall-effect sensor (A3517SUA, Allegro MicroSystems, Inc., Worcester, Massachusetts, USA) on one side of the joint, and a rare-earth magnet (6.35mm diam x 3.18mm, NdFeB, 10,800 Gauss strength, K&D Magnetics, Inc., Boca Raton, Florida, USA) on the other side. Joint motion changes the distance between the two, varying the sensor output. The sensors are wired to exposed connectors (2.5mm PC board header) for connection to external cables.

For actuation, each finger has a pre-stretched, nylon-coated stainless steel cable (7x7 strand core, 0.94mm diam, 540N breaking strength) anchored into the distal link. This cable runs through the bodies of the proximal and base links through low-friction nylon 11 tubing (3.2mm OD, 2mm ID). Due to the joint compliance the finger can be under-actuated, allowing for one tendon cable to drive both joints. A dovetail protrusion on the base link allows the finger to be securely connected to the grasper base.

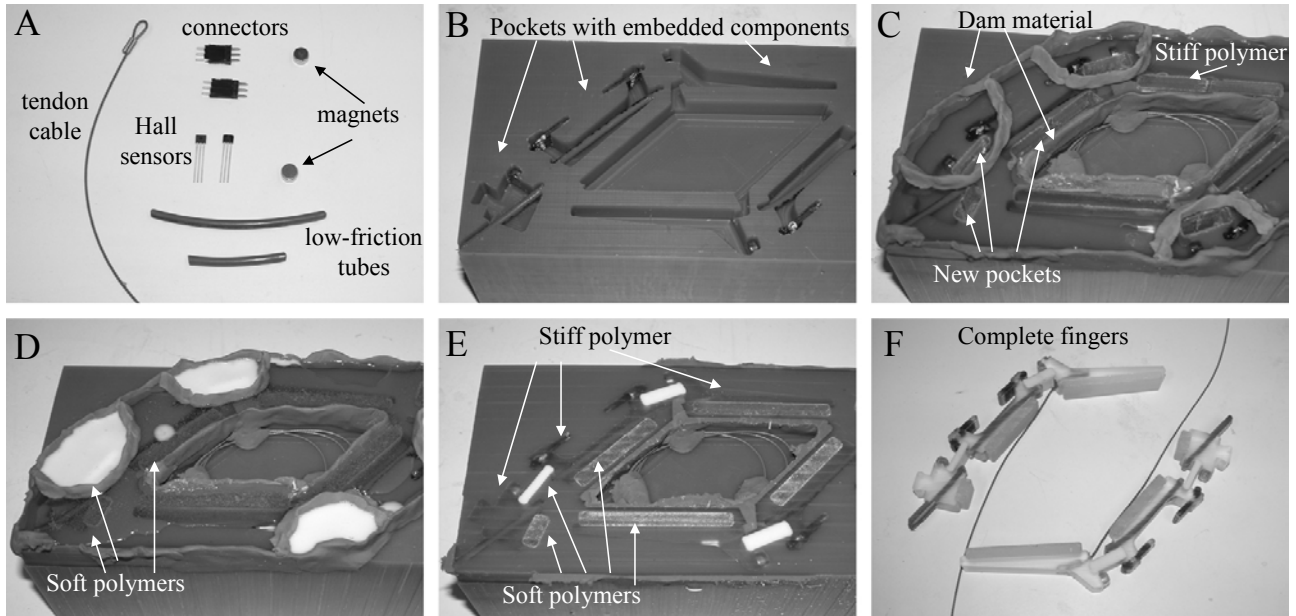


Fig. 2 Steps of the Shape Deposition Manufacturing (SDM) process used to fabricate the grasper fingers.

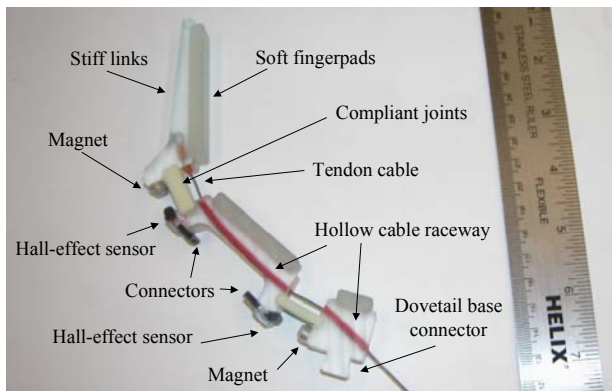


Fig. 3 Details of finger parts and placement of components.

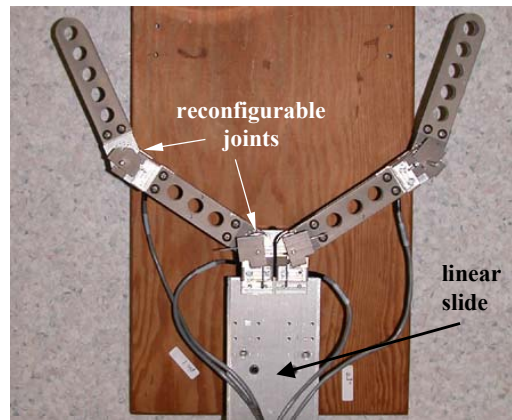


Fig. 5 Overhead view of the aluminum grasper.

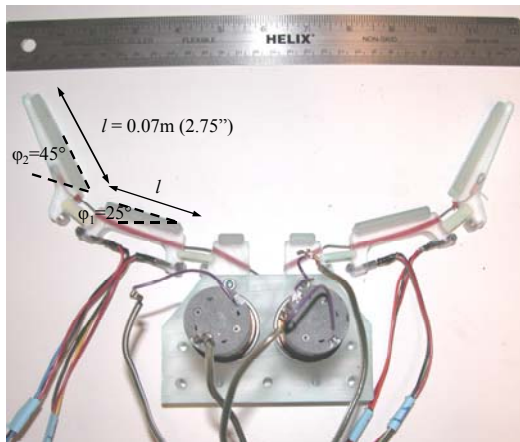


Fig. 4 Overhead view of the SDM grasper.

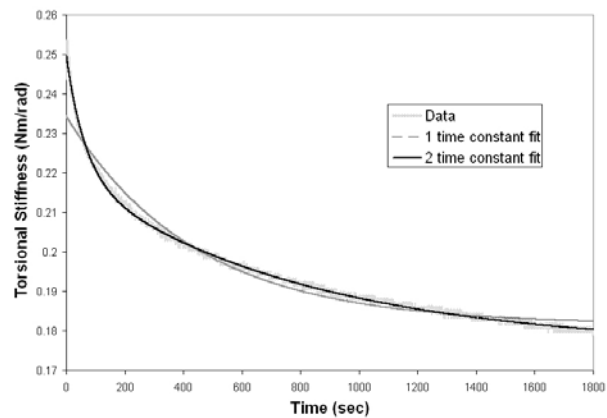


Fig. 6 Force relaxation of the distal joint of the SDM finger, for an angular step displacement of 0.5374 radians.

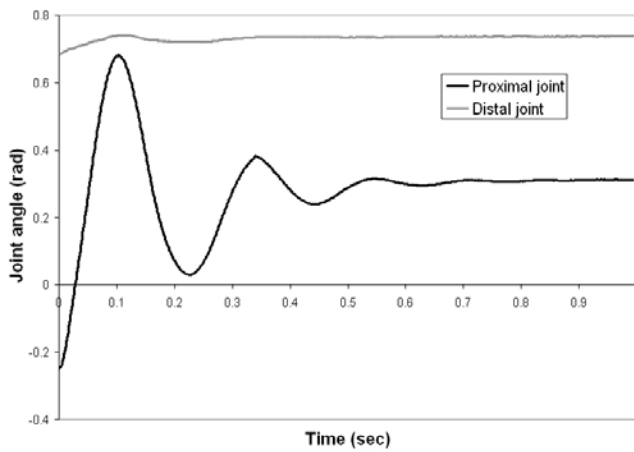


Fig. 7 Joint response of the SDM finger to a tip step displacement released at time=0.

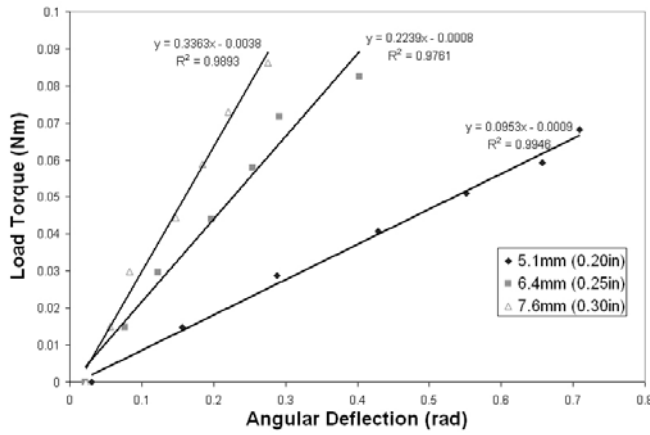


Fig. 8 Angular deflection of SDM joints as torque load is varied. Samples tested are 15.2mm (0.6in) long, 12.7mm (0.5in) deep, and varied in the direction of load application.

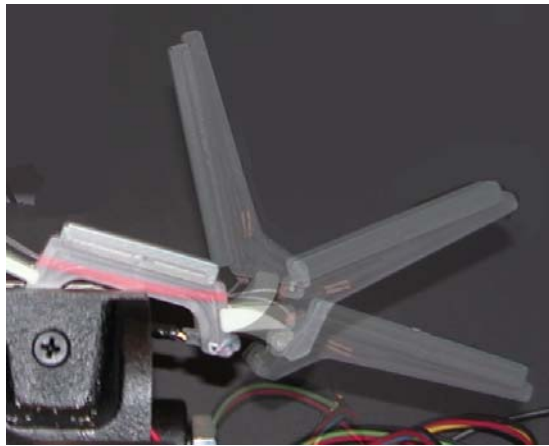


Fig. 9 Diagram of joint deflection and link motion for three positions across the travel range of the distal joint of the fingers

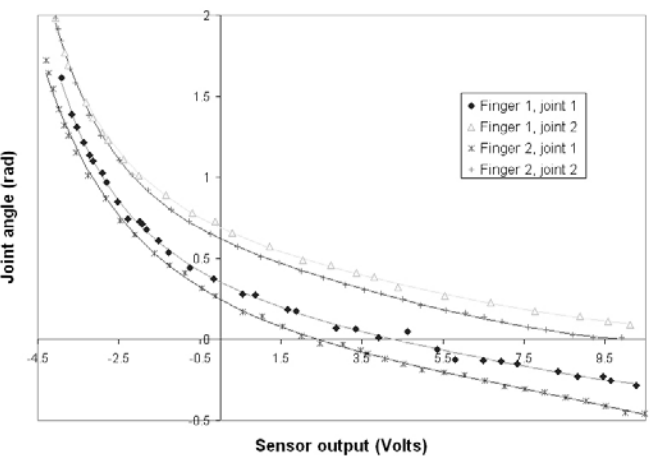


Fig. 10 Joint angle sensor calibration data and fits

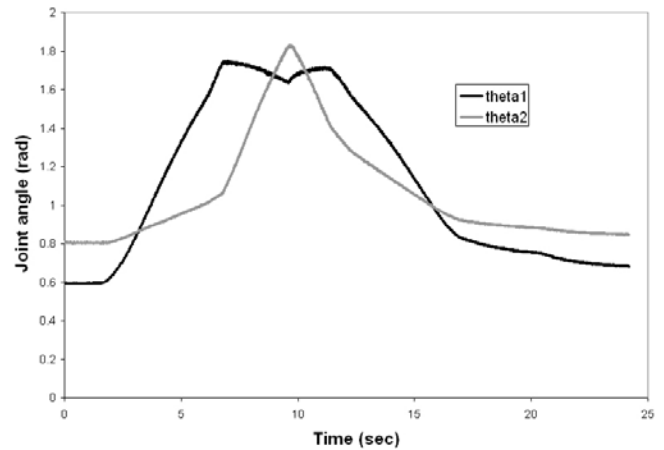


Fig. 11 Joint behavior as the finger is freely actuated.

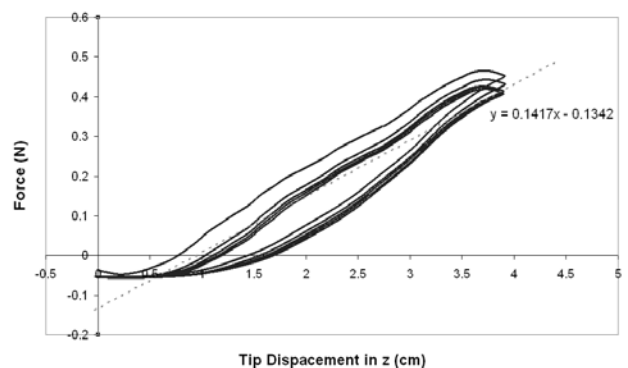


Fig. 12 Force-deflection curve of the tip of the SDM finger with linear trendline. The data represents five cycles of tip motion.

Figure 4 shows the fully assembled grasper (two fingers, two motors, and base). The base was also produced using SDM, but is purely structural. The link lengths, measured from the centers of the joint flexures, were chosen to be equal to enable the tip to reach the origin. The joint rest angles of the fingers (25 deg and 45 deg, for the proximal and distal joints, respectively) were carefully chosen based on the results of previous optimization studies [9,10]. The ratio of joint stiffnesses (0.19 proximal/distal) was chosen based on the optimization studies as well as material and geometric considerations to create a functional grasper. These angles and stiffnesses were shown to enable grasping of the widest range of object sizes with the greatest amount of uncertainty in object position.

The design is almost completely 2.5 dimensional (i.e. extruded 2 dimensional shapes) and symmetric about the center plane, allowing for the same finger to be used on the right or left side of the grasper.

For comparison to the single-part SDM finger, a similar grasper made from aluminum that was used in previous work is shown in Figure 5. Each finger on this grasper contains over 60 distinct parts, 40 of which are fasteners! The entire mechanism of the SDM fingers exists as one part. There is also a significant weight reduction in the SDM fingers (39g each) versus the aluminum fingers of similar size (~200g each).

#### Mechanism Behavior

A number of tests were performed to classify the behavior of the SDM grasper. The polyurethane used for these joints (IE90A) demonstrates significant viscoelastic behavior, as shown in Fig. 6. The sample tested corresponds to the dimensions of the distal joint flexure. A step angular displacement of 0.54 radians was applied, and the joint torsional stiffness was measured over a 30-minute interval.

The results show behavior consistent with a second-order Kelvin model, as shown in the figure [17]. Note the non-zero origin of vertical axis, chosen to highlight the goodness of curve fits. The second-order fit corresponds to the equation

$$k_\theta = 0.176 + 0.0303e^{-0.0156t} + 0.0437e^{-0.00125t}, \quad (1)$$

where  $k_\theta$  and  $t$  have units of (Nm/rad, seconds), respectively. Over the 30-minute time interval tested, the joint stiffness drops 29%. The time constants are much larger than typical grasp time, so the damping in the material has little effect on control of the grasper.

The viscoelastic properties of the joint material have the beneficial effect of damping out joint oscillations caused by grasper accelerations. In an undamped compliant grasper, these oscillations can be large due to the significant moment of inertia about the joints caused by long finger links, an effect we observed in our previous prototype (with music wire torsional springs in the joints) [10]. In this conventionally assembled grasper, oscillations due to large step displacements persisted for tens of seconds after release.

Low joint stiffness, although minimizing unwanted contact forces, increases the magnitude of resonant oscillations. Damping in the joints reduces the severity of these oscillations and therefore permits use of low joint stiffness. Figure 7 shows the joint response of the SDM finger to a large step

displacement of the fingertip, released at time=0. Note that the oscillations are unnoticeable after less than 1 second.

Figure 8 shows the torque, angular deflection behavior of the joints of the grasper for different joint flexure sizes. Loads were applied and removed quickly in order to minimize the effects of the material viscosity. Note that the joint angular deflections are nearly linearly proportional to load torque even across large deflections, allowing for the assumption of simple cantilevered-beam bending behavior.

Figure 9 shows the behavior of the finger joints through their range of motion. Note that the center of rotation varies slightly with joint angle. Figure 10 shows the output of the joint angle sensors (after amplification) and their fits versus joint deflection for the two fingers used in this study. The fit curves are of the form

$$\theta = (c_4 V^4 + c_3 V^3 + c_2 V^2 + c_1 V + c_0)^{-1} - 1, \quad (2)$$

where  $c_i$  are the fit coefficients and  $\theta$  and  $V$  have units of (radians, volts), respectively. These sensors give sufficient sensitivity across the entire range of motion of the joints to allow for use in the control of the grasper.

Note that the sensor gives better resolution as the finger opens ( $\theta$  gets smaller) in order to be more sensitive during passive contact under normal operation than when the grasper is actuated. This allows the grasper to be used as a “feeler”.

Figure 11 shows the joint deflection behavior as the finger is freely actuated (without object contact). Note that the distal joint moves very little until the proximal joint completes its full range of motion, due to differences in joint stiffness and cable lever arm. This behavior is similar to that of the two distal joints of the human finger, and increases the chances that both links of the finger are in contact with the object, increasing contact area and friction. The “dip” in the theta1 curve is caused by out-of-plane motion that occurs when a joint has reached its travel limit. The hall-effect sensors are only calibrated for motion in the plane.

Figure 12 shows the force generated at the tip of the fingers due to displacement in the out-of-plane direction ( $z$  direction following the convention of Fig. 13). The tip was displaced at a rate of approximately 1 cm/sec while mounted on an actuated linear slide mechanism (R2D series rodless actuator, Industrial Devices Corporation, Petaluma, CA). Force was measured with a multi-axis force/torque sensor (Gamma model, ATI Industrial Automation, Apex, NC). This data represents force generated due to motion of the tip across the tested range and back for a total of five cycles, low-pass filtered with a cut-off frequency of 1 Hz, to remove sensor noise. Note the hysteresis in the curves and the force relaxation due to viscoelasticity. The data is fitted with a trend line, to give an indication of the tip stiffness. The same tests were performed in the  $x$  and  $y$  directions (following the convention of Fig. 13) and show similar behavior. The approximate tip stiffness in the  $x$ ,  $y$ , and  $z$  directions are 5.85, 7.72, and 14.2 N/m, respectively.

The SDM fingers, while exhibiting very low tip stiffness, can also undergo large deflections while remaining completely functional. In the test shown in Fig. 12, the tip was displaced more than 3 cm in the out-of-plane direction without any degradation of mechanical properties. The advantages of this property are clear when considering the usual result of unplanned contact during use of traditional research hands.

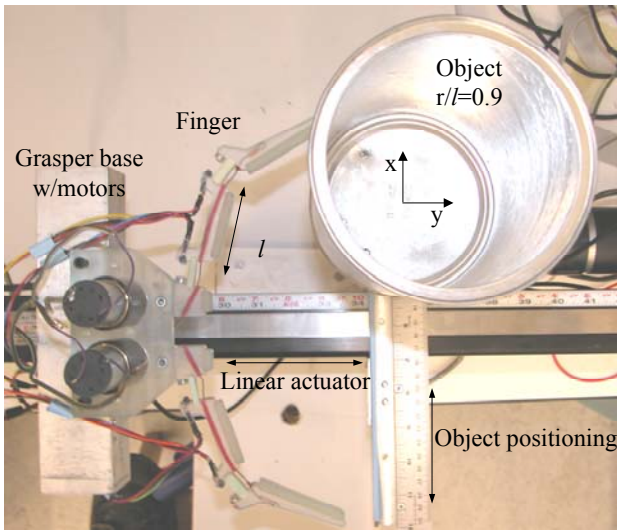


Fig. 13 Experimental setup. The grasper is mounted on an actuated linear slider and the object, affixed to a six-axis force/torque sensor, can be positioned at distances normal to the actuation direction.

The grasper does not exhibit this amount of compliance during all phases of the grasping task, however. Although not quantitatively evaluated, the grasper becomes much stiffer after it is actuated, a desirable characteristic allowing for more accurate manipulation of the grasped object. In the actuated mode, any compliance is due to compression of the joint flexures, as opposed to bending in the unactuated finger.

To give a sense of the robustness of the mechanism to impact loads, a more informal test was performed. An SDM finger was repeatedly dropped from a height of over 15m (50') onto a marble floor. After two attempts, no noticeable damage had occurred. After three, a small piece broke off of the dovetail connector. After six attempts, the outer link developed a large crack and one of the magnets broke off – but the sensors and joints remained completely intact and functional.

## EXPERIMENTAL EVALUATION

### *Experimental Apparatus and Procedure*

To evaluate the ability of the compliant grasper to successfully grasp objects in the presence of uncertainty in object location, we measured the range of object positions for which a successful grasp could be obtained. The grasper was mounted on a high precision, screw-driven linear positioner moving in the  $y$  direction, allowing the grasper to be brought into contact with the target object. The objects were positioned at increasing distances  $x_c$  from the center of the grasper in the lateral  $x$  direction, and securely mounted to prevent motion due to gripper-object contact forces. A diagram of the experimental apparatus is shown in Fig. 13. The objects were metal cylinders chosen to reflect the sizes used in previous studies [9,10], and were mounted on a multi-axis force/torque sensor (Gamma model, ATI Industrial Automation, Apex, NC) to record the contact forces in the plane. Due to the combined resolutions of the data acquisition system and the sensor, force was recorded at a resolution of 0.016N.

Joint angles and contact forces were recorded as the grasper was moved forward along the linear actuator at a rate of 2 cm/sec. Based on the joint angle information and knowledge

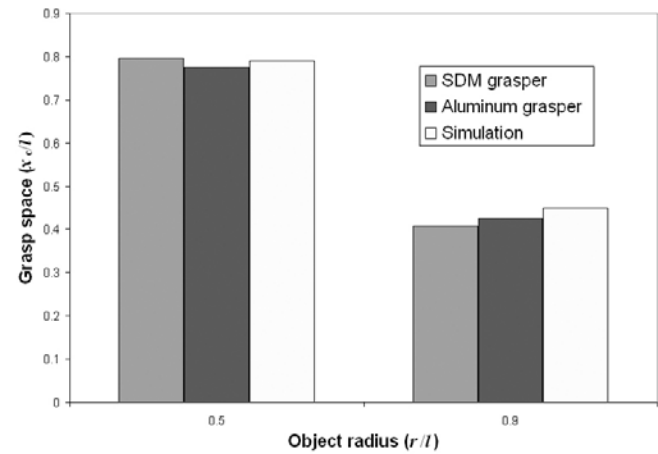


Fig. 14 Successful grasp range of the SDM grasper compared to the aluminum grasper and simulation.

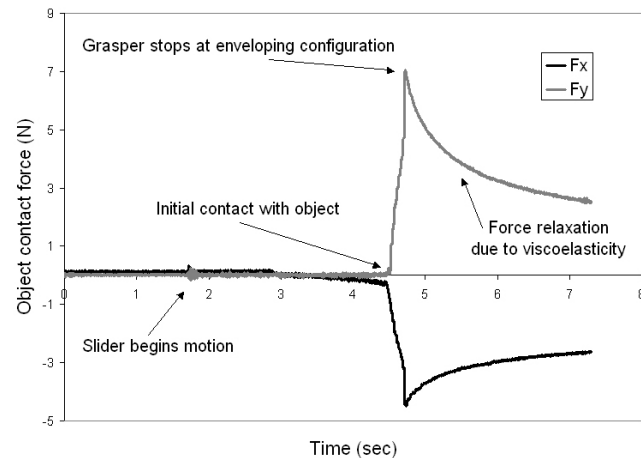


Fig. 15 Object forces due to grasper contact. Grasper moves forward at a constant velocity of 2 cm/sec until a successful grasp configuration is reached.

of the object size and distance from the line of travel, the amount of object enclosure was calculated using the kinematics of the grasper and geometry of the object. If the grasper finger contacts can enclose greater than 180 degrees of the object surface, an enveloping grasp will be attained, and the grasp is deemed successful. For this evaluation of grasp range, the grasper is not actuated, but is allowed to passively conform to the shape of the target object. The kinematics of the grasper and object pair determines grasp success. See [9,10] for a more in-depth discussion of this grasping scenario and success metric.

The performance of the grasper mechanism was evaluated for normalized object radius,  $r/l$ , and object location,  $x_c/l$ , incremented by 0.023 from the center toward the outside of the grasping range, where  $l$  represents the grasper link length. The maximum normalized distance of the object from the centerline for which a successful grasp was attained was recorded for each configuration. This value represents the successful grasp range and indicates the grasper's robustness to uncertainty in object location. The normalized contact forces,  $F_R l/k_T$ , applied to the object during the grasping process were also recorded for each tested value of object location,  $x_c/l$ .

## Results

Fig. 14 shows the successful grasp range of the SDM grasper and the analogous results from the aluminium grasper (Fig. 5) and simulation [9,10]. The object can be located anywhere within that range and be successfully grasped, indicating the allowable uncertainty in object position for a successful grasp. The grasp range was tested for  $r/l=0.5$  and  $r/l=0.9$ , with stiffness ratio  $k_1/k_2=5.3$ . The values of the SDM grasp range show good agreement with the aluminum and simulated graspers.

Figure 15 shows an example plot ( $r/l=0.9$  and  $x_c/l=0.45$ ) of the magnitude of object contact forces as the grasper moves forward against the object until a successful grasp configuration is obtained. Note the stages of the grasping process as reflected in the object forces.

## CONCLUSIONS AND FUTURE WORK

Passive compliance confers a number of advantages for robotic hands. Previous studies showed that carefully tuned joint compliance maximizes the range of object positions that result in a successful grasp, and minimize the magnitude of forces that the grasper applies to the object [9,10]. These benefits are particularly important in unstructured environments, where object location and size may be poorly known.

In this paper, we present a gripper fabricated using a simple prototyping technique that minimizes construction complexity and increases robustness, while preserving the advantages of passive joint compliance. Robustness is a limiting factor in experimental development of multifingered robot hands: the expense and fragility of these hands precludes casual experimentation, restricting the type of experimental tasks that can be reasonably attempted and slowing implementation due to the need for careful validation of programs. The grasper design presented here demonstrates that polymer-based Shape Deposition Manufacturing allows the construction of fingers with the functionality of conventional metal prototypes but far superior robustness properties.

We have described the design, fabrication, and evaluation of a compliant grasper that has properties desirable for grasping with inherent uncertainty: large successful grasp range, low passive contact forces due to mechanical compliance, and robust construction. However, the performance of the grasper has only been evaluated in structured tasks that foreshadow the performance in unstructured tasks. The natural extension of this work, therefore, is testing with more unstructured tasks, relaxing the assumptions of object geometry and position and the requirement of an enveloping grasp for grasp success. We plan to test the grasper as an end-effector on the Whole-arm Manipulator (WAM, Barrett Technologies, Cambridge, Massachusetts, USA) to provide a flexible testbed for future studies.

There are also further design improvements to implement. The first is creating a non-planar grasper by adding and reconfiguring finger locations. Planned improvements to finger design include greater stiffness out-of-plane, optimized configuration and placement of tendons, and implementation of contact and force sensing.

## ACKNOWLEDGMENT

The authors would like to thank Mark Cutkosky, Moto Hatanaka, and Miguel Piedrahita for their advice and assistance with implementing the SDM process. Also, we would like to thank Chris Johnson for all of his work in setting up, testing and debugging the process.

This work was supported by the Office of Naval Research grant number N00014-98-1-0669.

## REFERENCES

- [1] K. J. Salisbury, "Active stiffness control of a manipulator in Cartesian coordinates," *19<sup>th</sup> IEEE Conf. Decision and Control*, pp..95-100, 1980.
- [2] M. R. Cutkosky and I. Kao, "Computing and controlling the compliance of a robotic hand," *IEEE Transactions on Robotics and Automation*, vol. 5 (2), pp. 151-165, 1989.
- [3] J. P. Desai and R. D. Howe, "Towards the development of a humanoid arm by minimizing interaction forces through minimum impedance control," *Proceedings of the 2001 IEEE Int. Conf. on Robotics and Automation*, pp. 4214-4219, 2001.
- [4] J. Loncaric, "Geometrical analysis of compliant mechanisms in robotics," Ph.D. thesis, Harvard University, 1985.
- [5] D. E. Whitney, "Quasi-static assembly of compliantly supported rigid parts," *Journal of Dynamic Systems, Measurement, and Control*, vol. 104, pp. 65-77, 1982.
- [6] J. M. Schimmels and S. Huang, "A passive mechanism that improves robotic positioning through compliance and constraint," *Robotics and Computer-Integrated Manufacturing*, vol. 12 (1), pp. 65-71, 1996.
- [7] L. Biagiotti, F. Lotti, C. Melchiorri, G. Vassura, "Mechatronic design of innovative fingers for anthropomorphic robot hands," *Proceedings of the 2003 IEEE International Conference on Robotics and Automation*, pp. 3187 -3192, 2003.
- [8] S. Hirose and Y. Umetani, "Soft gripper," *Proceedings of the 1983 ISIR*, pp. 112-127, 1983, cited in M. Kaneko, T. Tsuji, M. Ishikawa, "The robot that can capture a moving object in a blink," *Proceedings of the 2002 IEEE International Conference on Robotics and Automation*, pp. 3643-3648, 2002.
- [9] A. M. Dollar and R. D. Howe, "Towards grasping in unstructured environments: Optimization of grasper compliance and configuration," *Proceedings of the 2003 IEEE/RSJ International Conference on Intelligent Robots and Systems (IROS 2003)*, Las Vegas, NV, October 27-31, 2003.
- [10] A. M. Dollar and R. D. Howe, "Towards grasping in unstructured environments: Grasper compliance and configuration optimization," *Advanced Robotics*, vol. 19(5), pp. 523-544, 2005.

- [11] R. Merz, F. B. Prinz, K. Ramaswami, M. Terk, L. Weiss, "Shape Deposition Manufacturing," *Proceedings of the Solid Freeform Fabrication Symposium*, University of Texas at Austin, August 8-10, 1994.
- [12] M. Binnard and M. R. Cutkosky, "A Design by Composition Approach for Layered Manufacturing," *ASME Transactions, J. Mech. Design*, vol. 122, no. 1, pp 91-101, 2000.
- [13] J. E. Clark, J. G. Cham, S. A. Bailey, E. M. Froehlich, P. K. Nahata, R. J. Full, M. R. Cutkosky, "Biomimetic design and fabrication of a hexapedal running robot," *Proceedings of the 2001 International Conference on Robotics and Automation*, Seoul, Korea, 2001.
- [14] B. H. Park, M. Shantz, F. B. Prinz, "Scalable rotary actuators with embedded shape memory alloys," *Proceedings of SPIE, The International Society for Optical Engineering*, vol. 4327, pp. 79-87, 2001.
- [15] K. B. Shimoga, A. A. Goldenberg, "Soft materials for robotic fingers," *Proceedings of the 1992 IEEE International Conference on Robotics and Automation*, pp. 1300-1305, 1992.
- [16] M. R. Cutkosky, J. M. Jourdain, P. K. Wright, "Skin materials for robotic fingers," *Proceedings of the 1987 IEEE International Conference on Robotics and Automation*, pp. 1649-1654, 1987.
- [17] Y. C. Fung, "Biomechanics: Mechanical properties of living tissues," Springer-Verlag, 2<sup>nd</sup> edition, 1993.